Al-Nahrain Journal of Science
ANJS, Vol.27(2), June, 2024, pp. 114-118

Plastic Optical Fiber Sensor for Sensing Refractive Index of Citric Acid Based on Surface Plasmon Resonance

Ghufran Mohammed Jassam[1,*], Zeinah K. Abdaldeen[1], Reem M. Taboor[1], Sara M. Ibraheim[1], Aida Benchaabane[2]

[1]Department of Pysics, College of Science, Al-Nahrain University, Jadiriya, Baghdad, Iraq
[2]Aviation School of Borj El Amri, Science and Technology for Defense Laboratory, Military Research Center, Military Academy, Tunis, Tunisia.

Article's Information

Received: 19.04.2024
Accepted: 14.05.2024
Published: 15.06.2024

Keywords:
Citric acid
Surface Plasmon resonance
Plastic optical fiber
Optical fiber sensor

Abstract

Using plastic optical fiber with multimode (MPOF), an optical fiber sensor (OFS) based on Surface Plasmon Resonance (SP.R) was created and put into use. The sensor is used to determine performance metrics including signal to noise ratio (SNR), Sensitivity (S), Figure of merit (FOM), and Resolution(R) in addition to detecting and measuring the refractive index of different concentrations of citric acid. With a sensing region exposed to 50 nm of gold (Au) metal layer, the optical fiber-based SPR sensor was found to have a sensitivity value of 1250nm, an SNR of 0.27, a figure of merit of 93.3 and a resolution 8×10^{-4}.

http://doi.org/10.22401/ANJS.27.2.11
*Corresponding author: ghufran.muhammed@nahrainuniv.edu.iq

1. Introduction

Glass or plastic fibers are examples of optical fibers. The idea of total light reflection permits light waves to propagate via optical cables with minimal loss. Optical fiber is widely used in practical applications such as optical sensors and optical communication [1]. Novel photonic sensors have also been developed as a result of advancements in fiber optics and optoelectronics technology. These sensors are simple to use, offer real-time information, and, in certain cases, perform better than their electronic equivalents. Intensity, evanescence, spectrum, and interference via fiber optic sensors are the main types of these sensors [2]. In addition to accounting for the disadvantages of traditional detection techniques, optical fiber sensors offer a number of benefits including great durability, corrosion resistance, remote control, online monitoring, low cost, easy operation, anti-electromagnetic interference, and high sensitivity [3, 4]. Optical fiber sensors using surface plasmon resonance are one of the most notable types of optical fiber sensors. This is due to the numerous benefits of SPR technology: Real-time detection, temperature self-calibration, high refractive index sensitivity, high refractive index resolution, and no requirement for label sampling [5]. As a result, SPR technology has been used in numerous domains, including biochemistry [6], optoelectronics [7], etcetera. Surface plasmon resonance SPR-based analytical sensors are incredibly sensitive to molecular interactions at the metal-dielectric interface [5]. SPR sensors based on prisms in particular Make complete use of the characteristics that enable the detection of tiny changes in the amplitude or phase of reflected light, which can be used to discriminate between analytes that are near to metal [8,9]. Surface Plasmon waves (SPWs) are created when a sample and a thin layer of reflecting metal (such as gold or silver) are linked by use of a highly refractive substrate [10,11]. It happens when surface Plasmon Resonance (SPR) and polarized light undergo a large-scale oscillation of density at a metal-die electrical interface below the appropriate phase [12–14]. An optical sensor established on SPR can be utilized for applications such as biomedical and chemical diagnostics, environmental safety, electrochemistry sciences, and life sciences [15, 16]. This work aimed at sensing and calculating the refraction value of citric acid by using the grade plastic optical fiber sensor established on SPR.

2. Materials and Methods

The dimensions of the multimode optical plastic fiber are as follows: diameter of 1000µm, a core of 980µm, a numerical aperture of 0.51 µm and cladding of 20µm. Within a block of resin, plastic optical fiber was placed, and the D-shaped waveguide was created by turning off half of the diameter of the plastic fiber padding. A polishing technique was then applied. To remove the cladding components and core, 5µm polishing paper was used in the polishing process. Following a Figure of "8," as seen in Figure 1, after 20 complete strikes. The polishing process was then carried out. After the removed clad portion had been cleaned with distilled water, sputtering was used to deposit gold metal with a thickness of around 50 nm. Gold was used because it is chemically neutral. The sputtering process schematic diagram appears in Figures 1 and 2 for the treated grade plastic optical fiber. Table 1 presents the gold coating parameter as displayed on the Quorum screen (150 RES).

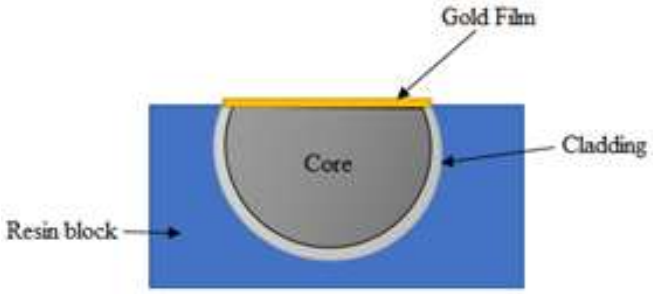

Figure 1. Cross section of the system sensor.

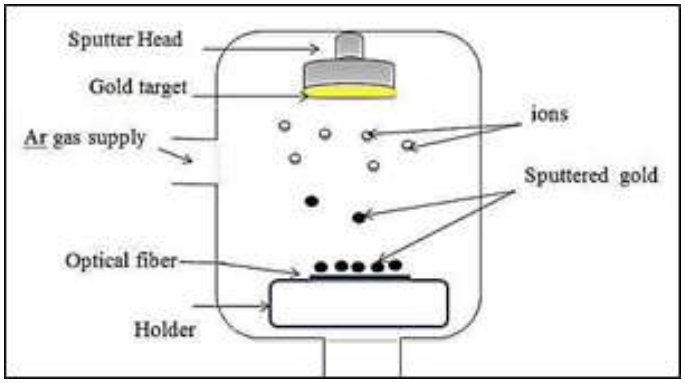

Figure 2. The schematic diagram of sputtering process.

Table 1. The Specification of the Quorum- Q 150R ES sputtering apparatus.

The vacuum chamber's diameter	165 mm
Present range	1-80 mA
Time range for spraying	1-3600 sec

Using a very practical experimental setup that is inexpensive and simple to use, highlights the layer metal efficiency in this configuration. The optical spectrum analyzer, a plastic optical fiber, and a light source of a halogen torch made up the experimental setup. A computer is linked to the OSA. As demonstrated in Figures. 3 and 4, the SPR bends and data can be seen and stored online.

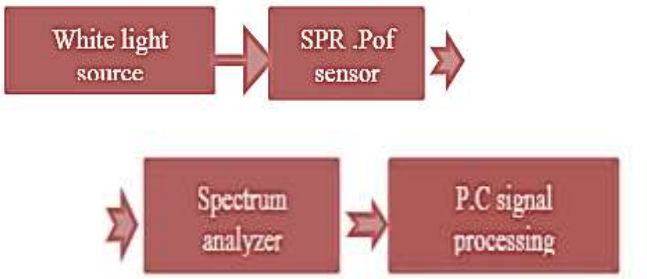

Figure 3. The overview of the plastic optical fiber experiment

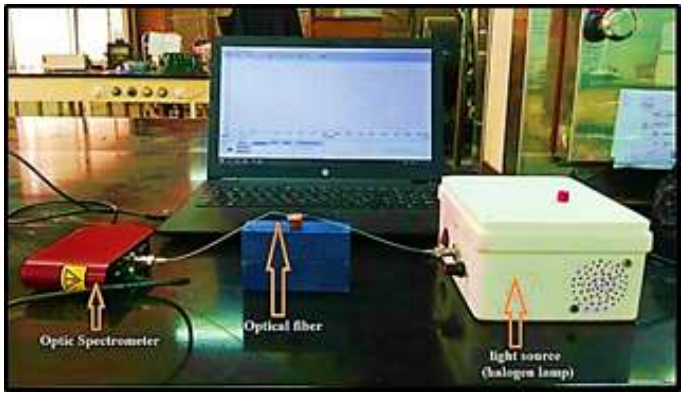

Figure 4. The experimental setup of the surface Plasmon resonance.

.

3. Performance Parameters for surface Plasmon Resonance

Performance characteristics to be studied include sensitivity, signal-to-noise ratio, figure of merit, and resolution. In the case of spectral interrogation, sensitivity can be defined as the change in resonance wavelength per unit change in the refractive index of the sensing medium, and it can be written as [17]:

$$S = \frac{\Delta\lambda_{res.}}{\Delta n_s} \quad \ldots (1)$$

where $\Delta\lambda_{res}$ and Δn_s are the change of the resonance wavelength and the change of refractive index, respectively. From this equation, the unit of the sensitivity is nanometers per refractive index unit in nm/RIU. Signal to noise ratio (SNR) and

figure of merit (FOM) are inversely proportional to the width of SPR spectral curve and can be written as [17]:

$$SNR(n) = \left[\frac{\Delta\lambda_{res.}}{\Delta\lambda_{0.5}}\right] \quad ...(2)$$

where $\Delta\lambda_{0.5}$ is the width of the spectral curve.

$$FOM = \frac{S}{\Delta\lambda_{0.5}} \quad ...(3)$$

The resolution of the sensor can be defined as the minimum of change in refractive index that is detectable by the sensor, and is given as [18]:

$$R = \frac{\Delta n_s}{\Delta\lambda_{res.}} \Delta\lambda_{RD} \quad ...(4)$$

where $\Delta\lambda_{DR}$ is the spectral resolution of the spectrometer.

3. Results and Discussion

In the numerical experiment, the following parameters were used: numerical aperture of optical fiber (N.A=0.51), core diameter of fiber D = 980 µm; L = 10 mm for the longitude detection, thickness of metal layer d = 50 nm gold; Varied solutions of sucrose/water with varying concentrations and thus varied (ns) refractive indices shield the sensor's sensitive area. A refractometer was used to determine the solution's refractive index (Abbe). The correlation between the solution concentration and refractive index is displayed in Figure 5.

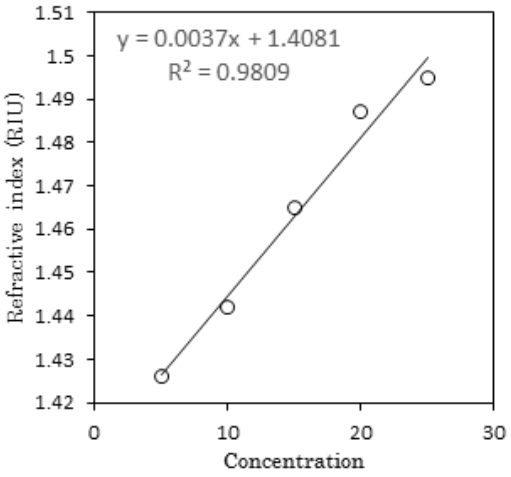

Figure 5. The sucrose solution's refractive index varies with the concentration of the solution.

And various values (1.34, 1.351, 1.354, 1.361 and 1.37) for the sucrose-water solution's refractive index. The proportion of the measured intensity (I) when using an optical connection and a sample, The amplitude of the optical signal (Io) obtained in the air was utilized to produce the spectra and record the light propagation curves T (transmission). The wavelength in nanometers (nm) determines the transmittance (T). The SPR curve is referred to as the wavelength curve or the resonance wavelength at a specific wavelength. Since the light energy at the incident is transferred to the metal's electron and reduces the intensity of reflected light, there is a noticeable, sudden dip in T. The refractive index (n) of the sensing medium determines this dip position. The resonance wavelength increases as the solution's refractive index increases. This phenomenon occurs due to a loss in energy, as shown in Figure 6, which results in the sudden dip in the sine wavelength being transferred to the sine wavelength side, or redshift.

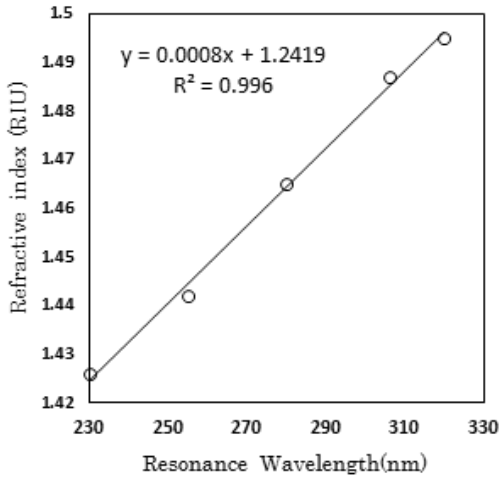

Figure 6. The refra.ctive index considering resonance wavelength.

Figure 7 displays the surface Plasmon resonance of the gol,d (Au) layer at particular refracctive index values of the citric acid sample sensiing de.vices. Since every sample has a distinct refractive index, it is clear that each SPR re,.sponse curve's width and dip position vary depending on the sensor. Additionally, as Adjusted SPR curve with width, the magnitude of the sh.if..ting increases. These modifications take place as a result of variations in the spectral curve's breadth, refractive index, and resonance wavelength that affect performance characteristics. As the sensing medium's refractive index and resonance wavelength shift, so do the shifting's value and the dip's location. When the refractive index RI of the detected region rises, the resonance wavelength abruptly falls and moves toward longer wavelengths (redshift). The resonance wavelength will sharply decline when the energy diminishes, shifting to the longer wavelength side as a result redshift.

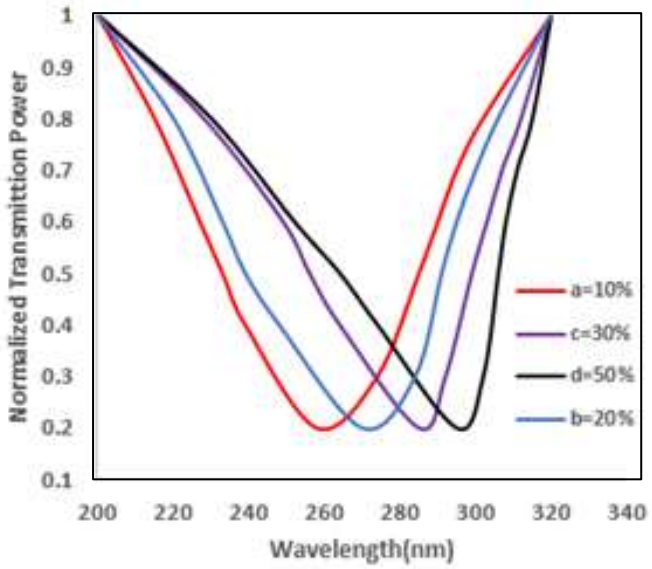

Figure 7. SPR curve of the layer metal (gold) optical fiber sensor for various citric acid samples: **(a)** Citric acid concentration 10%, **(b)** Citric acid concentration 20%, **(c)** c Citric acid concentration 30%, and **(d)** Citric acid concentration 50%.

The experimental performance parameters for the manufactured and simulated layer (gold) sensor are presented in Table 2. Table 3 provides the concentration and values for the refractive index for each citric acid at various wavelengths of reflection. Longer wavelengths are used for resonance because the refractive index rises with solution concentration. According to (Table 3), the resonant wavelength for each concentration is determined, and thus the refractive index for each sample is determined through (Figure 7).

Table 2. The Performance parameters based on surface plasmon of the gold layer.

Metal	Sensitivity (S) $(\mu m/RIU)$	Signal to noise ratio (SNR)	Figure of merit (FOM)	Resolution [RIU]
Gold	1250	0.27	93.9	$8x10^{-4}$

Table 3. Different Resonance wavelengths of citric acid samples and different values of refractive index.

Type of Fiber	Samples	(λ_{res})	Refractive Index(n)
	A	258	1.4483
	B	270	1.4579
Plastic OF	**C**	285	1.4699
	D	295	1.4779

4. Conclusions

In this work, we have reported the ability of a low-cost (SPR-POF) sensor to be exploited in chemical applications. The systems of (SPR_POF) sensor are easy to use, of small size and low cost. The change in the SPR response curves for each sample was reported which showed a dip in the resonance position. For each increase in the refractive index and thus for various values of the concentration of citric acid, a variation in the resonance wave occurs. This dip shift occurs for different types of solutions. The sensitivity of the resonance of plastic optic fibre-based surface Plasmon, with the 50 nm thick Au multi-layer of metal film exposed sensing region, had a value of 1250 nm/RIU, while the signal-to-noise ratio was 0.27.

Funding: No funding is received for this work.

Conflicts of Interest: The authors declare no competing interests

References

[1] Lobry, M.; Lahem, D.; Loyez, M.; Debliquy, M.; Chah, K.; David, M.; Caucheteur, C.; "Non-enzymatic D-glucose plasmonic optical fiber grating biosensor". Biosens. Bioelect., 142: 111506, 2019. https://doi.org/10.1016/j.bios.2019.111506

[2] Mustafa, H.N.; Soudad, S.A.; "Coreless optical fiber for hemoglobin (HB) sensing with bilayer based on surface plasmon resonance". J. Opt., 52(4): 1724-1729, 2023. https://doi.org/10.1007/s12596-022-00999-6

[3] Loyez, M.; Lobry, M.; Hassan, E.M.; DeRosa, M.C.; Caucheteur, C.; Wattiez, R.; "HER2 breast cancer biomarker detection using a sandwich optical fiber assay". Talanta, 221: 121452, 2021. https://doi.org/10.1016/j.talanta.2020.121452

[4] Ravi, K.; Rana, T.; Banshi, D.G.; "A highly sensitive and distinctly selective D-sorbitol biosensor using SDH enzyme entrapped Ta2O5 nanoflowers assembly coupled with fiber optic SPR". Sen. Actu. B: Chemical, 242: 810-817, 2017. https://doi.org/10.1016/j.snb.2016.09.178

[5] Monireh B.; Adil, D.; "Highly sensitive detection of Cd (II) ions using ion-imprinted surface plasmon resonance sensors". Microchem. J., 159: 105572, 2020. https://doi.org/10.1016/j.microc.2020.105572

[6] Wei, L.; Zhihai, L.; Yu, Z.; Song, L.; Yaxun, Z.; Xinghua, Y.;Jianzhong, Z.; Libo, Y.; "Specialty optical fibers and 2D materials for sensitivity

enhancement of fiber optic SPR sensors: A review". Opt. Las. Technol., 152: 108167, 2022. https://doi.org/10.1016/j.optlastec.2022.108167

[7] Zhao, Y.; Lei, M.; Liu, S. X.; Zhao, Q.; "Smart hydrogel-based optical fiber SPR sensor for pH measurements". Sen. Actu. B: Chemical, 261: 226-232, 2018. https://doi.org/10.1016/j.snb.2018.01.120

[8] Yusoff, S.F.A.Z.; Mezher, M.H.; Amiri, I.S.; Ayyanar, N.; Vigneswaran, D.; Ahmad, H.; Zakaria, R.; "Detection of moisture content in transformer oil using platinum coated on D-shaped optical fiber ". Opt. Fib. Tech., 45: 115-121, 2018. https://doi.org/10.1016/j.yofte.2018.07.011

[9] Murtadha, F.S.; Abbas, K.A.; Firas, S.M.; "Design and simulation of localized surface plasmon resonance-based fiber optic chemical sensor". IOP Conference Series: Mater. Sci. Eng., 871: 012074, 2020. https://doi.org/10.1088/1757-899X/871/1/012074

[10] Wang, Q.; Ren, Z.H.; Zhao, W.M.; Wang, L.; Yan, X.; Zhu, A.S.; Zhang, K.K.; "Research advances on surface plasmon resonance biosensors". Nanoscale, 14(3): 564-591, 2022. https://doi.org/10.1039/D1NR05400G

[11] Haidar, J.M.; Shaymaa, H.K.; Duaa, A.T.; "Ag/CdS surface plasmon simulation systems for gas sensor". Kuwait J. Sci., 50(3): 216-222, 2023. https://doi.org/10.1016/j.kjs.2023.05.007

[12] Ghufran, M.J.; Soudad, S.A.; "High sensitivity for toxic metal ion sensor based on tapered PCF Mach–Zehnder interferometer". J. Opt., 53: 1079-1085, 2023. https://doi.org/10.1007/s12596-023-01197-8

[13] Murtadha, F.S.; Ali, A.A.; Shehab, A.K.; "Surface plasmon resonance based fiber optic sensor: theoretical simulation and experimental realization". Al-Nahrain J. Sci., 21(1): 65–70, 2018. https://doi.org/10.22401/JUNS.21.1.11

[14] Ghufran, M.J.; Soudad, S.A.; "The effect of tapered photonic crystal fiber structure on the performance of Mach–Zehnder interferometer to detection of toxic metal ion (Zinc)". J. Opt. **52**(2): 683-690(2023). https://doi.org/10.1007/s12596-022-01023-7.

[15] Ghufran, M.J.; "Acetic acid concentration estimation using plastic optical fber sensor based surface plasmon resonance". Iraqi J. Phys, 17(43): 11–17 2019. https://doi.org/10.20723/ijp.17.43.11-17

[16] Ravindran, N.; Kumar, S.; Yashini, M.; Rajeshwari, S.; Mamathi, C.A.; Nirmal, T.S.; and Sunil, C.K.; "Recent advances in Surface Plasmon Resonance (SPR) biosensors for food analysis: A review". Crit. Rev. Food Sci. Nutr., 63(8): 1055-1077, 2023. https://doi.org/10.1080/10408398.2021.1958745

[17] Nunzio, C.; Davide, M.; Laura, C.; Luigi, Z.; "Low cost sensors based on SPR in a plastic optical fiber for biosensor implementation". Sensors, 11(12): 11752-11760,2011. https://doi.org/10.3390/s111211752.

[18] Sachin, K.S.; Banshi, D.G.; "Influence of ions on the surface plasmon resonance spectrum of a fiber optic refractive index sensor". Sensors and Actuators B: Chemical, 156(2): 559-562,2011. https://doi.org/10.1016/j.snb.2011.01.068.